JOURNAL OF VIROLOGY, Sept. 2006, p. 8961–8969 Vol. 80, No. 18
0022-538X/06/$08.00+0 doi:10.1128/JVI.00843-06

Adeno-Associated Virus Type 2 Contains an Integrin α5β1 Binding Domain Essential for Viral Cell Entry

Aravind Asokan,[1] Julie B. Hamra,[1] Lakshmanan Govindasamy,[2] Mavis Agbandje-McKenna,[2] and Richard J. Samulski[1]*

Gene Therapy Center, University of North Carolina at Chapel Hill, Chapel Hill, North Carolina 27599,[1] and Department of Biochemistry and Molecular Biology, College of Medicine, University of Florida, Gainesville, Florida 32610[2]

Received 24 April 2006/Accepted 7 June 2006

Integrins have been implicated as coreceptors in the infectious pathways of several nonenveloped viruses. For example, adenoviruses are known to interact with αV integrins by virtue of a high-affinity arginine-glycine-aspartate (RGD) domain present in the penton bases of the capsids. In the case of adeno-associated virus type 2 (AAV2), which lacks this RGD motif, integrin αVβ5 has been identified as a coreceptor for cellular entry. However, the molecular determinants of AAV2 capsid-integrin interactions and the potential exploitation of alternative integrins as coreceptors by AAV2 have not been established thus far. In this report, we demonstrate that integrin α5β1 serves as an alternative coreceptor for AAV2 infection in human embryonic kidney 293 cells. Such interactions appear to be mediated by a highly conserved domain that contains an asparagine-glycine-arginine (NGR) motif known to bind α5β1 integrin with moderate affinity. The mutation of this domain reduces transduction efficiency by an order of magnitude relative to that of wild-type AAV2 vectors in vitro and in vivo. Further characterization of mutant and wild-type AAV2 capsids through transduction assays in cell lines lacking specific integrins, cell adhesion studies, and cell surface/solid-phase binding assays confirmed the role of the NGR domain in promoting AAV2-integrin interactions. Molecular modeling studies suggest that NGR residues form a surface loop close to the threefold axis of symmetry adjacent to residues previously implicated in binding heparan sulfate, the primary receptor for AAV2. The aforementioned results suggest that the internalization of AAV2 in 293 cells might follow a "click-to-fit" mechanism that involves the cooperative binding of heparan sulfate and α5β1 integrin by the AAV2 capsids.

Integrins comprise a large family of heterodimeric cell surface receptors that mediate biological processes related to cell signaling, adhesion, motility, and communication (16). In addition to these diverse roles, integrins have been exploited by a number of viral and bacterial pathogens to gain entry into host cells (41). In nonenveloped viruses, capsids often bind receptors through projections or indentations on the surfaces that readily enable the mimicking of native multimeric ligands (3, 14). For example, the vitronectin binding αVβ3 and αVβ5 integrins are internalization receptors for human adenovirus (Ad) (28). Following the initial attachment via prominent homotrimeric fibers, Ad is rapidly internalized into clathrin-coated vesicles. This is thought to be mediated by penton base association with integrin αVβ3 and αVβ5 through an exposed RGD motif. The fivefold symmetry of the Ad penton base promotes the formation of an integrin ring structure that may play a key role in mediating virus internalization (4, 37). Other examples of the role of integrins in viral cell entry are the rotavirus, which is known to utilize integrins α2β1, α4β1, and αVβ3 for infecting intestinal cells (12, 13), and the foot-and-mouth disease virus, which utilizes an RGD motif similar to that of Ad in binding αVβ1, αVβ3, and αVβ6 integrins (17, 18, 19).

Adeno-associated virus (AAV) is a nonpathogenic human parvovirus with a single-stranded DNA genome encapsidated in an icosahedral shell of about 25 nm in diameter (2). Capsid proteins of AAV are viral protein 1 (VP1), VP2, and VP3, with molecular masses of 87, 73, and 62 kDa, respectively, with VP3 forming the major structural component of the virion shell (33). Of the several serotypes and variants that have been identified, AAV serotypes 1 to 9 are currently being developed as gene therapy vectors (11). The diverse tissue tropism(s) of these serotypes is thought to stem from their ability to exploit a variety of primary and secondary receptors for transduction. For example, AAV2 has been shown to utilize heparan sulfate (39) and AAV1, -4, -5, and -6, which display different tropisms than that of AAV2, utilize sialic acid with different linkage specificities for cell surface binding (20; Z. Wu and R. J. Samulski, unpublished data). Although the initial cell surface binding of viral capsids is often mediated through cell surface glycosaminoglycans, many viruses require more than one receptor to facilitate infection (36). In addition, AAV also appears to utilize several coreceptors, such as fibroblast growth receptor 1 and hepatocyte growth receptor by AAV2 (21, 31) and platelet-derived growth receptor by AAV5 (5), for successful cellular entry.

Our lab and others have previously shown that integrin αVβ5 serves as a coreceptor for AAV2 infection (34, 38). In this report, we demonstrate that AAV2 utilizes α5β1 as an alternative coreceptor in 293 cells, which lack αVβ5 integrin (see reference 26 and references therein). More importantly, we have identified a putative tripeptide integrin recognition sequence within the VP3 capsid component of AAV2, which appears to be conserved in a majority of AAV serotypes. Molecular modeling studies suggest that this integrin binding domain forms a surface loop located at the threefold axis of

* Corresponding author. Mailing address: CB No. 7352, Gene Therapy Center, 7113 Thurston Building, The University of North Carolina at Chapel Hill, Chapel Hill, NC 27599-7352. Phone: (919) 962-3285. Fax: (919) 966-0907. E-mail: rjs@med.unc.edu.

symmetry adjacent to residues previously implicated in binding heparan sulfate, the primary receptor for AAV2. Our findings support the notion that efficient infection of 293 cells by AAV2 is mediated by a sequential process involving capsid binding to cell surface heparan sulfate, followed by α5β1 integrin. The formation of higher-order molecular complexes achieved through the cooperative binding of primary and secondary receptors by AAV could in turn trigger coordinated events that are essential for cellular entry.

MATERIALS AND METHODS

Plasmids, viral vectors, and biochemical reagents. The AAV2/R513A mutant (mut) was generated by site-directed mutagenesis of the pXR2 plasmid (32) using the QuikChange multisite-directed mutagenesis kit (Stratagene, La Jolla, CA). The oligonucleotide primer 5′-CCA AGT ACC ACC TCA ATG GCG CAG ACT CTC TGG TGA ATC CGG-3′ was synthesized at the nucleic acid core facility at University of North Carolina (UNC)—Chapel Hill. Wild-type (wt) or mutant pXR2 plasmid containing AAV2 Rep and Cap genes, pXX6-80 containing adenovirus helper genes, and pTR-CMV-FLuc containing the firefly luciferase gene driven by the cytomegalovirus promoter were utilized for vector production using the triple-plasmid transfection protocol developed in our lab (47). Viral genome titers were determined using a dot blot hybridization method with a radiolabeled luciferase transgene probe (32). All monoclonal antibodies (MAbs) targeted against integrin α and β subunits and the soluble α5β1 integrin receptor formulated in octylglucoside were purchased from Chemicon (Temecula, CA). Bromodeoxyuridine (BrdU) was purchased from Sigma (St. Louis, MO).

Cell culture. The HEK 293 cell line used in the production of AAV vectors and other experiments described herein was obtained from the UNC vector core and maintained in Dulbecco's modified Eagle's medium (DMEM) supplemented with 10% fetal bovine serum (FBS) and penicillin-streptomycin (100 U/ml). The CHO-derived integrin α5-negative (CHOB2) and α5-reconstituted cell lines (CHOB2α27) were kind gifts from Rudy Juliano. The heparan sulfate-negative CHOpgsD cell line was obtained from the American Type Culture Collection (Manassas, VA). All CHO-derived cell lines were maintained in α-MEM supplemented with 10% FBS, penicillin-streptomycin (100 U/ml), ribonucleosides, and deoxyribonucleosides. The CS1 and CS1/β5 cell lines were kind gifts from David Cheresh with permission from Caroline Damsky. These cells were maintained in suspension with DMEM supplemented with 10% FBS and penicillin-streptomycin (100 U/ml).

Solid-phase heparin binding studies. The abilities of the wt AAV2 and AAV2/R513A mutant to bind heparan sulfate, the natural receptor of AAV2, were determined as follows. Heparin-conjugated agarose beads (500 μl; Sigma, St. Louis, MO) were loaded onto Micro BioSpin columns (Bio-Rad, Hercules, CA) and washed three times with 1× phosphate-buffered saline (PBS). Purified wt/mut AAV2 particles (10^{10} vector genomes) were then loaded onto the column, followed by the collection of flowthrough, three washes with PBS, and eluate fractions at different salt concentrations. The quantification of vector genomes that eluted in different fractions was carried out by dot blot hybridization.

Solid-phase integrin binding studies. The ability of the R513A mutation to impair the binding of AAV2 capsids to the soluble nondenatured form of integrin α5β1 was performed as follows. Soluble integrin α5β1 (5 μg/ml) was patterned on a nitrocellulose membrane in a 96-well format using a dot blot manifold. The membrane was then washed with PBS, blocked with 10% milk in PBS, and incubated with wt or mutant AAV2 capsids in 5% nonfat milk in PBS for 30 min at room temperature. Following three washes with PBS at room temperature, the membrane was washed and probed with A20 primary antibody (1:20 dilution in 2% milk) against AAV2 capsids for 30 min. The membrane was then washed and incubated with anti-mouse horseradish peroxidase-conjugated secondary antibody (Pierce, Rockford, IL; 1:7,500 dilution in 2% milk) for 30 min, and the relative binding intensities were quantified by chemiluminescence and densitometric analysis.

Cell adhesion studies. The abilities of wt AAV2 and AAV2/R513A mutant capsids to inhibit the adhesion of HEK 293 cells to fibronectin, the natural ligand for integrin α5β1, were compared with those of monoclonal antibodies against several integrin receptors. Briefly, confluent 15-cm plates of 293 cells were split and allowed to recover in FreeStyle 293S (Invitrogen, Carlsbad, CA) suspension medium overnight. Cells (~5×10^4) were then incubated with wt/mut AAV capsids at a high multiplicity of infection (MOI) (~10^6) or anti-α5β1, anti-αVβ3, anti-αVβ5 antibodies (20 μg/ml) for 1 h at 37°C to facilitate receptor internalization/blockade. The cells were plated on fibronectin-coated 96-well plates (Bio-Rad, Hercules, CA) in quadruplicate and allowed to adhere for 30 min at 37°C. Wells were washed three times with PBS and fixed with 4% paraformaldehyde in PBS for 5 min at room temperature (RT). Subsequently, 100 μl of crystal violet dye solution (0.5% wt/vol dissolved in 20% ethanol in PBS) was added to each well, incubated for 15 min at RT, and washed three times with PBS and the cells were incubated with 0.1% Triton X-100 for several hours at RT. The quantification of dye uptake in 293 cells adhered to fibronectin-coated wells was performed using UV absorbance spectroscopy (λ_{max} = 595 nm).

Cell surface binding and internalization studies. The ability of the AAV2/R513A mutant or wt AAV2 to bind to the surface of HEK 293 cells was determined as follows. Briefly, wt or mutant AAV2 capsids were incubated with 10^7 cells in suspension medium (MOI, 1,000) for 2 h at 4°C to allow cell surface binding. Cells were then washed three times with PBS, and half of the samples were incubated at 37°C for 1 h to allow internalization. The latter half of the samples were then washed with PBS and spun down at 13,000 × *g* for 1 min, and the cell pellet was resuspended in 100 μl trypsin-EDTA (Sigma, St. Louis, MO) for 5 min at room temperature. Cells were then washed three times with PBS and all cell-associated vector/genomic DNA was extracted using a DNeasy kit (QIAGEN). The quantification of AAV genomes bound to the cell surface or internalized in 293 cells was achieved by dot blot hybridization used previously in determining vector genome titers.

Viral transduction assays. All transduction assays were performed by quantifying luciferase transgene expression in cell lysates at 24 h postinfection with D-luciferin (NanoLight, Pinetop, AZ) as the substrate using a Victor2 luminometer (PerkinElmer, Wellesley, MA). For inhibition studies, HEK 293 cells were preincubated with monoclonal antibodies against different integrin α and β subunits (20 μg/ml) for 1 h at 37°C to facilitate receptor blockade. In addition, 293 cells were treated with AAV2 capsids (MOI, 1,000) preincubated with soluble integrin α5β1 (20 μg/ml) for 1 h on ice, followed by the quantitation of luciferase transgene expression 24 h postinfection. The CS1 cells were pretreated with BrdU (2 μM) for 48 h to promote the overexpression of integrin subtypes (40). Subsequently, wt AAV2-Luc or AAV2/R513A-Luc vectors (MOI, 1,000) were incubated with treated cells at 37°C in the continued presence of inhibitors/chemicals for 24 h prior to the quantification of luciferase expression. The CS1/β5 cell line and CHO-derived cell lines were also incubated with wt or mut AAV vectors (MOI, 1,000) at 37°C, and the transduction efficiencies were assessed at 24 h postinfection.

Animal experiments. Transduction efficiencies of wt AAV2 and the AAV2/R513A mutant in vivo (dose 10^{10} vector genomes) were determined, following intramuscular administration into the hind limbs of male BALB/c mice (6 to 8 weeks of age), by quantifying luciferase transgene expression using the Xenogen IVIS 100 imaging system. Animals were imaged 3, 7, 14, 21, and 28 days postinjection with a single intraperitoneal administration of D-luciferin (120 mg/kg). All protocols were approved by the IACUC at UNC—Chapel Hill.

Molecular modeling. The location of the asparagine-glycine-arginine (NGR) integrin recognition sequence on the VP3 domain of the AAV2 capsid was determined by generating a three-dimensional model of a VP3 trimer using VIPER (viperdb.scripps.edu), with the available coordinates of AAV2 (48; PDB accession no. 1LP3) supplied as a template. Subsequent surface rendering and mapping of the NGR loop was performed using PyMOL (www.pymol.org).

RESULTS

Alternative integrin receptor for AAV2 in HEK 293 cells. HEK 293 cells are known to lack integrins αVβ3/β5 but contain αV/α5β1 integrins (see reference 26 and references therein). As shown in Fig. 1, monoclonal antibodies targeted against integrin subunits α5, β1, or the α5β1 heterodimer significantly inhibit the transduction of wt AAV2-Luc in 293 cells. In contrast, anti-αV and anti-αVβ5 antibodies fail to inhibit AAV2 transduction in this cell line. Further, coincubation of the AAV2 capsid with the soluble α5β1 integrin receptor results in an approximately 50% inhibition of luciferase transgene expression in 293 cells. These results support the notion that α5β1 integrin can serve as a coreceptor for AAV2 infection in 293 cells, which lack αVβ5 integrin. The aforementioned observations are analogous to adenovirus type 5, which utilizes αVβ1 as an alternative coreceptor in the absence of integrin αVβ3 for infection in 293 cells (26).

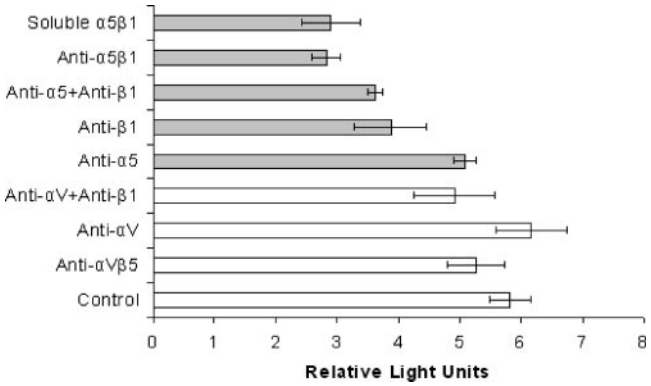

FIG. 1. Anti-integrin antibody-mediated inhibition of AAV2 transduction in 293 cells. Cells grown in 24-well plates (10^5/well) were incubated for 1 h at 37°C with monoclonal antibodies (20 μg/ml) targeted against different integrin subunits and heterodimers. The cells were then dosed with AAV2-Fluc (MOI, 1,000) in the continued presence of MAbs at 37°C for 24 h prior to the quantitation of luciferase transgene expression in cell lysates. Soluble integrin α5β1 (1 μg/ml) was preincubated with AAV2-Fluc particles for 1 h on ice, and 293 cells were incubated with the mixture for 24 h at 37°C prior to that quantitation of luciferase expression. All experiments were performed in triplicate. Gray bars depict statistically significant data in comparison with the control ($P < 0.05$). Error bars indicate standard deviations.

Scanning the AAV capsid for integrin α5β1 recognition sequences. Several integrin binding motifs have been identified in the literature through mutagenesis and phage display studies (23, 24, 25, 30). Among these, the high-affinity RGD motif and the moderate-affinity NGR motif previously identified in fibronectin and isolated in phage display studies are well known. Scanning the capsid protein sequences of AAV serotypes for such motifs and subsequent sequence alignment revealed an NGR motif at positions 511 to 513 in the VP3 regions of a majority of AAV serotypes (Fig. 2). Based on these findings, we performed site-directed mutagenesis to elucidate the potential role of this NGR motif in AAV capsid-integrin interactions. Briefly, the AAV2/R513A mutant was engineered using a site-directed mutagenesis kit to present an NGA motif instead of the wt NGR domain proposed to be involved in integrin binding. This mutant AAV vector was generated successfully by using the triple-plasmid transfection protocol, and the genomic titers were not significantly impacted by this mutation (~2.5-fold less than those of wt AAV2 vectors).

Interaction of the R513A mutant with heparin and soluble integrin α5β1. The heparin binding profile of the AAV2/R513A mutant was compared with that of wt AAV2. As shown in Fig. 3A, the elution profiles for wt and mut AAV2 determined by dot blot hybridization are identical, with both vectors

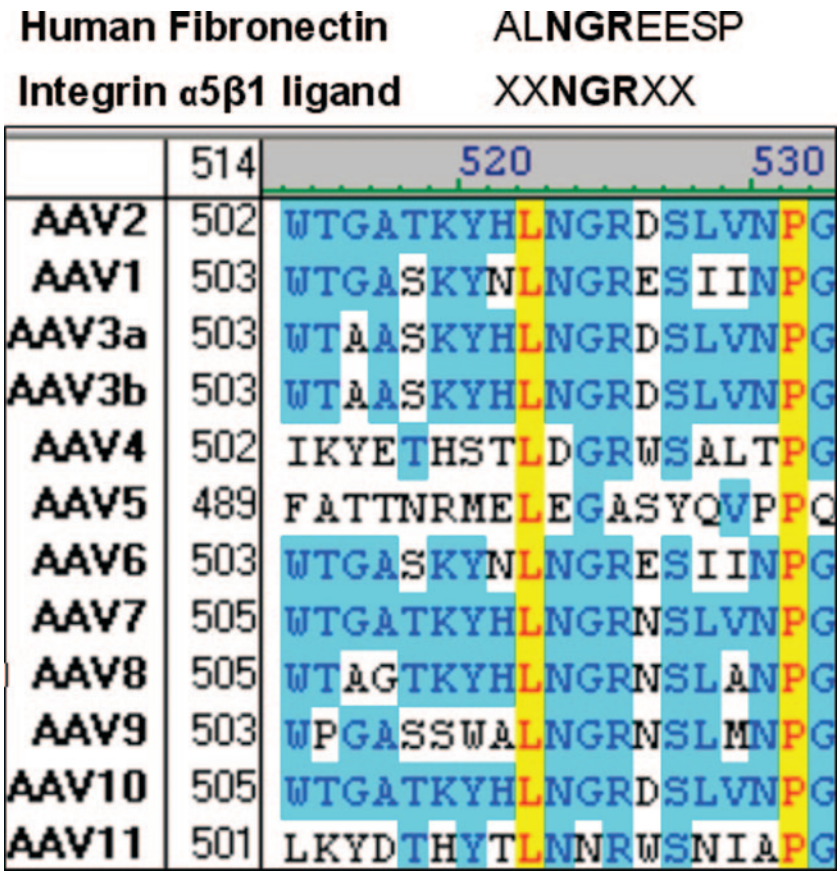

FIG. 2. Sequence alignment of the NGR motif found in the 9th type III repeat of fibronectin (25), integrin α5β1 binding NGR domain identified through phage display (23, 24), and a partial section of the VP3 region of AAV serotypes performed in vector NTI. The 511-NGR-513 domain is conserved in the majority of AAV serotypes except AAV4, -5, and -11. AAV4 contains an inverse RGD (DGR) motif, also previously identified as a low-affinity integrin binding motif. Similar residues are depicted with a black font/blue background, dissimilar residues with a black font/white background, and conserved residues in with a red font/yellow background.

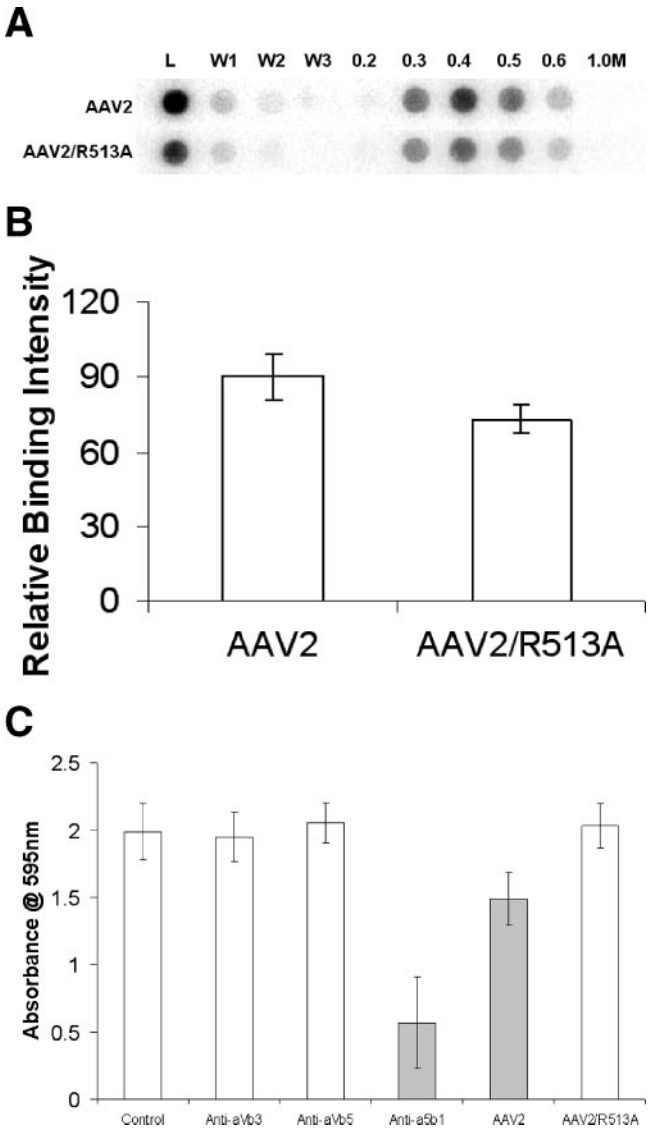

FIG. 3. (A) Heparin binding profiles of wt and mut AAV2 particles. Heparin-conjugated agarose beads (500 μl) were loaded in MicroSpin columns, and viral particles (~10^{10}) were allowed to bind the beads for about 10 min at room temperature. Flowthrough, washes (1× PBS), and eluates at different salt concentrations (in PBS) were collected, and the number of vector genomes in each fraction was determined by dot blot hybridization. Experiments were performed in duplicate. (B) Solid-phase integrin α5β1 binding profiles of wt AAV2 and mut AAV2/R513A capsids. Soluble integrin α5β1 (1 μg/ml) was embedded in nitrocellulose membranes under nondenaturing conditions and probed with either wt or mut AAV2 particles in 5% milk, followed by A20 MAb (1:20 dilution), which recognizes intact AAV2 particles. The extent of binding was quantitated with a horseradish peroxidase-conjugated secondary antibody by using chemiluminescence and densitometric analysis ($n = 3$; $P < 0.05$). (C) Competitive inhibition of 293 cell adhesion to fibronectin-coated substrates. Confluent 293 cells were trypsinized and allowed to recover overnight in suspension culture medium. Cells were then incubated with MAbs against integrins α5β1, αVβ3/β5 (20 μg/ml), wt AAV2, or the AAV2/R513A mutant (MOI, ~10^8) at 37°C for 1 h to facilitate receptor internalization/blockade. Treated and untreated cells were then allowed to adhere to fibronectin-coated plates for 30 min, fixed, and treated with crystal violet solution (0.5% wt/vol in 20% ethanol in PBS). Cell adhesion was quantitated by determining the UV absorbance of each sample at 595 nm. Gray bars indicate statistically significant data compared with that of the control ($n = 4$, $P < 0.05$). Error bars indicate standard deviations.

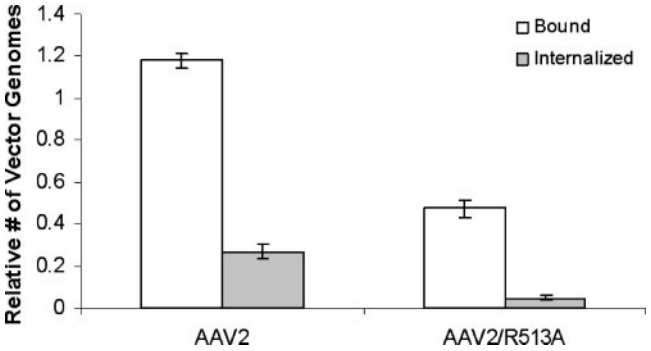

FIG. 4. Cell surface binding of wt and mutant AAV2 particles. Viral particles were allowed to bind 293 cells for 1 h at 4°C. The cells were then washed three times with 1× PBS, and total cell-associated DNA was extracted using a DNeasy kit. Vector genomes associated with 293 cells were quantitated by dot blot hybridization. All experiments were performed in triplicate. The mutant displayed a statistically significant decrease ($P < 0.05$) in binding integrin α5β1 and the surface of 293 cells in comparison with that of wt AAV2. Error bars indicate standard deviations.

eluting at a peak fraction of 0.4 M NaCl. These results suggest that the R513A mutation does not alter the heparin binding affinity of AAV2. Further, in order to demonstrate the potential interaction between the proposed NGR motif and integrin α5β1 in a cell-free setting, we determined the ability of the R513A mutant to bind the soluble integrin α5β1 embedded in a nitrocellulose membrane. As shown in Fig. 3B, the R513A mutant displays a modest decrease in its ability to bind solid-phase integrin α5β1 compared to that of wt AAV2. A potential explanation for these observations is the likelihood that both AAV2 and integrin α5β1 might require functional activation to adapt their respective high-affinity conformations (15, 38, 43).

Competitive inhibition of fibronectin-integrin α5β1 interactions. The ability of wt AAV2 and AAV2/R513A mutant capsids to inhibit the adhesion of HEK 293 cells to a fibronectin-coated substrate was compared with that of monoclonal antibodies against several integrin receptors. As seen in Fig. 3C, the anti-α5β1 integrin antibody, but not the anti-αVβ3/β5 antibodies, was able to block 293 cell adhesion to fibronectin-coated wells by nearly 75%, thereby validating the expression of the fibronectin receptor in this cell line. In competitive inhibition studies with viral capsids, wt AAV2 capsids were able to block 293 cell adhesion by approximately 25%. In contrast, the adhesion of 293 cells to fibronectin in the presence of the R513A mutant was essentially similar to that of the control, implying that mut AAV2 capsids are unable to engage integrin α5β1 and compete for fibronectin binding.

Cell surface binding and internalization of the R513A mutant in 293 cells. Binding and cell entry of the R513A mutant were compared with those of wt AAV2 in 293 cells, which express constitutive levels of heparan sulfate proteoglycans and integrin α5β1 (6, 26). As seen in Fig. 4, the amount of mutant AAV2/R513A bound to the surface of 293 cells is 2.5-fold less than the amount of wt AAV2. In addition, approximately 10% of surface-bound mutant R513A capsids are internalized into 293 cells in contrast to surface-bound wt AAV2, 25% of which are internalized at 1 h postinfection. Such reduced cell surface binding and internalization of

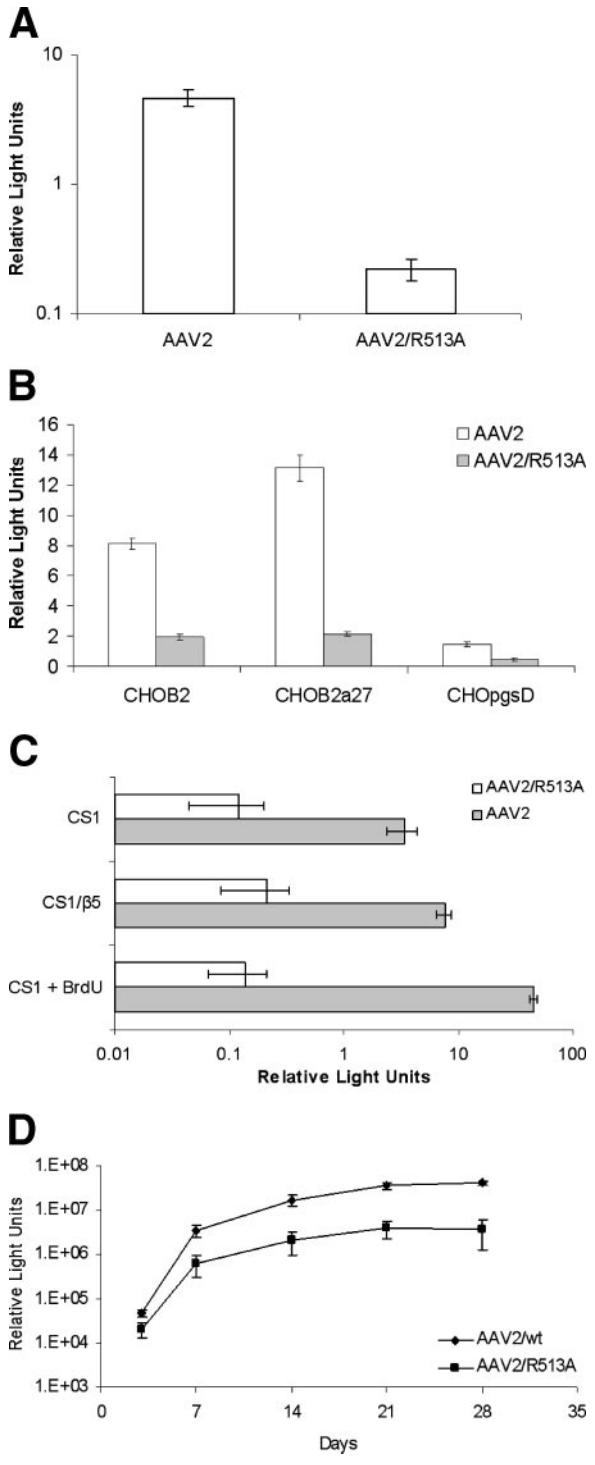

FIG. 5. In vitro transduction profiles (luciferase transgene expression) of wt and mut AAV2 vectors (MOI, 1,000) in (A) 293 cells; (B) CHOB2 (integrin α5 negative), CHOB2α27 (integrin α5 transfected), and CHOpgsD (heparan sulfate negative) cells; and (C) CS1 cells before or after treatment with BrdU (2 μM) at 24 h postinfection. Statistical significance was established at $P < 0.05$ ($n = 6$). (D) In vivo transduction profiles of wt and mut AAV vectors (dose 10^{10} vector genomes per mouse) following intramuscular administration into the hind limbs of male BALB/c mice. Images of luciferase transgene expression in vivo were obtained using the Xenogen IVIS 100 imaging system and quantified using Living Image (version 2.5) software. Statistical significance was established with $P < 0.05$ ($n = 4$). Error bars indicate standard deviations.

AAV2/R513A in 293 cells might arise due to the need for cooperative binding of heparan sulfate as well as integrin α5β1 by AAV2 capsids for efficient cell entry (see Discussion for details).

Transduction studies with the AAV2/R513A mutant. The effect of the R513A mutation on the transduction efficiency of AAV2 in different cell types was determined by quantifying luciferase transgene expression at 24 h postinfection. As shown in Fig. 5A, transgene expression in 293 cells transduced with the R513A mutant was an order of magnitude lower than that obtained with the wt AAV2 vector. To understand this transduction-deficient phenotype further, the transduction efficiency of the AAV2/R513A mutant was monitored in different CHO cell lines exhibiting specific receptor phenotypes. The CHOB2 cell line was isolated based on its inability to bind fibronectin and lacks a functional integrin α5β1 receptor (35). The CHOB2α27 cell line expresses a full-length human α5 subunit with 27 amino acids in the cytoplasmic domain and is capable of binding fibronectin to an extent similar to that of wild-type CHO cells (1). As shown in Fig. 5B, the ability of wt AAV2 to transduce CHOB2α27 cells is significantly enhanced compared with that of CHOB2 cells. Interestingly, the AAV2/R513A mutant does not display a similar enhancement in transduction efficiency despite the restoration of functional α5β1 integrin subunits in the CHOB2 cell line. These results indirectly support the notion that the NGR motif is a requisite for integrin α5β1-mediated transduction by AAV2.

The CHOpgsD cell line is defective in heparan sulfate biosynthesis and therefore does not express cell surface heparan sulfate (7, 8). Both wt and mutant AAV2 display reduced transduction efficiency in CHOpgsD cells. More importantly, the R513A mutant continues to display a significantly lower transduction compared to that of wt AAV2 in this heparan sulfate-deficient CHO cell line. These results further support the notion that the R513 residue is involved in interactions other than heparan sulfate binding and is critical for AAV2 transduction.

Similar transduction studies were performed with CS1 cells, which express immature forms of the integrin α5/αV subunits and low levels of integrin β1 (10, 40). The treatment of these cells with BrdU has been shown to promote the adhesion of cells to substrates, such as fibronectin and vitronectin, due to overexpression of multiple cell surface integrin heterodimers (40). As shown in Fig. 5C, the transduction of CS1 cells by wt AAV2 is dramatically enhanced upon pretreatment with BrdU. However, such an increase is not seen with the AAV2/R513A mutant despite the enhanced cell surface expression of multiple integrin subunits. In addition, the transduction efficiency of the R513A mutant remains unchanged compared to that of wt AAV2 in the CS1/β5 cell line, which was previously transfected with the human integrin β5 subunit (10, 44). These results further support the notion that the NGR motif is critical for integrin-mediated transduction of different cell types by AAV2 and might be required for interaction with alternative integrin receptors as well. Lastly, the defective phenotype of the R513A mutant is also seen upon the injection of the mutant in skeletal muscles of BALB/c mice. As shown in Fig. 5D, the AAV2/R513A mutant demonstrates a slower onset as well as lower level of luciferase gene expression in muscle tissue compared to those of wt AAV2. While these data correlate

well with results from in vitro studies, the impaired transduction of the R513A mutant in skeletal muscle in vivo might arise due to several factors, including its inability to exploit integrin receptors and/or possibly other steps in the trafficking pathway, such as uptake, endosomal escape, uncoating, and nuclear entry. In this regard, further experiments to characterize the roles of integrins in AAV infection in vivo are warranted.

DISCUSSION

Integrin α5β1 is a coreceptor for AAV2 infection. Multiple integrins have been implicated in the cellular entry pathways of nonenveloped viruses such as adenovirus and rotavirus (28, 36, 41). The HEK 293 cell line, which is commonly utilized in the propagation of adenovirus and the production of AAV vectors, is efficiently transduced by AAV2. These cells lack αVβ5, a previously identified coreceptor for AAV2 infection (38). In this study, we first demonstrate that integrin α5β1 can serve as an alternative coreceptor for AAV2 in 293 cells. Among other parvoviruses, erythrovirus B19 is known to utilize integrin α5β1 for entry into erythroid progenitor cells (43). Despite the expression of α5β1 and αVβ5 heterodimers in HeLa or A549 cells, monoclonal antibodies against αVβ5, but not α5β1, are capable of inhibiting AAV2 transduction in these cell lines (A. Asokan and R. J. Samulski, unpublished data). Based on these findings, it is likely that AAV2 exploits specific integrins in different cell lines during the course of infection. Mapping integrin receptor usage by AAV serotypes other than AAV2 could shed light on alternative pathways of AAV infection.

AAV contains a putative integrin α5β1 recognition sequence. The molecular determinants of integrin binding and subsequent cell entry by AAV have not been determined thus far. Previous phage display studies aimed at isolating a peptide ligand for integrin α5β1 have consistently identified the well-known, high-affinity RGD motif or a lower-affinity NGR domain (23, 24). The NGR sequence occurs in the 9th type III repeat of the cell binding region of fibronectin and could contribute to the interaction of fibronectin with the α5β1 integrin receptor (23, 24, 25). Scanning the AAV2 capsid for such integrin recognition sequences revealed an NGR motif at positions 511 to 513 in the VP3 region of AAV2. The NGR domain is highly conserved except in the cases of AAV4, AAV5, and AAV11. Interestingly, AAV4 has a DGR motif (inverse of RGD) previously shown to be a low-affinity integrin binding domain (23).

Based on the three-dimensional structure of AAV2, the NGR domain is located adjacent to R585 and R588 (Fig. 6A), which were previously implicated in heparin binding by AAV2 (22, 29). Closer examination of the protein folds reveals that the NGR domain forms a loop between two small beta strands and is partially exposed on the surface of the AAV2 capsid (Fig. 6B). A preliminary biochemical characterization of AAV2/R513A revealed that mutant and wt AAV2 particles possess similar heparin binding affinities (Fig. 3A). These results are corroborated by two previous reports that have separately established that an arginine-to-alanine point mutation at the 513 position in the AAV2 capsid does not affect heparin binding (22, 29).

Interestingly, the recognition of R513A particles eluted from the heparin column by the A20 antibody, which binds intact AAV2 capsids (45), was diminished in comparison to that of wt AAV2 particles postelution (data not shown). These results suggest that the R513A mutant, unlike wt AAV2, might undergo an irreversible conformational change subsequent to heparin binding. Based on these observations, it is tempting to speculate that conformational changes subsequent to heparan sulfate binding could result in a greater exposure of the NGR loop region for interaction with cell surface integrin receptors. Such a scenario is also plausible with other AAV serotypes, wherein capsid binding to their corresponding primary receptors, such as sialic acid, might trigger conformational changes that facilitate binding of the conserved NGR domain to integrin receptors.

The NGR motif is critical for AAV2 capsid-integrin interactions. The NGR integrin binding motif was previously identified through phage display studies (23, 24). Both the NG RAHA and fibronectin-derived ALNGREESP peptides were found to inhibit the binding of fibronectin to solid-phase integrin α5β1, albeit with moderate efficiency. Accordingly, the ability of the R513A mutant to competitively inhibit 293 cell adhesion to fibronectin-coated wells or bind solid-phase integrin α5β1 is only moderately impaired in comparison with that of wt AAV2 (Fig. 3B and C). Such modest differences between the abilities of wt AAV2 and mutant AAV2/R513A particles to interact with soluble integrin α5β1 were also seen during competitive inhibition studies with integrin binding peptides (data not shown). However, these modest differences become more pronounced in a cellular setting, wherein the R513A mutation impedes cell surface binding as well as uptake of AAV2 particles (Fig. 4). Therefore, it is likely that the R513A mutation precludes capsid interactions with integrin α5β1, thereby blocking cell entry. Further characterization of AAV2 capsid-integrin interactions through cryo-electron microscopy and studies with other AAV serotypes might provide structural insight into the exact nature of the interaction between the NGR domain and integrins. However, such studies are beyond the scope of this report.

The NGR motif is critical for α5β1 integrin-mediated AAV2 transduction. The R513A mutant displays reduced transduction efficiencies in different cell types in vitro and mouse skeletal muscle in vivo (Fig. 5). Such a transduction-deficient phenotype could arise due to the inability of the mutant capsid to bind cell surface receptors, which in turn affects the efficiency of cellular uptake. The reduced transduction of heparan sulfate-deficient CHOpgsD cells by the R513A mutant supports the involvement of receptors other than heparan sulfate in AAV2 cell entry. These conclusions are supported by the observation that reconstituting integrin subunits by transfection or overexpression of multiple integrin heterodimers by BrdU treatment in Chinese hamster cells fails to rescue the defective phenotype (Fig. 5B and C). These results support the notion that the NGR motif might facilitate capsid interactions not only with integrin α5β1 but also with alternative integrin receptors. It is noteworthy to mention that similar chemical treatment with phorbol myristoyl acetate has been utilized to induce α5β1 integrin activity in K562 leukemia cells (43). Such high-affinity conformation of integrin was found to enhance the transduction efficiency of parvovirus B19 in the presence of conformation-stabilizing antibodies.

At this juncture, it is noteworthy to mention the effect of

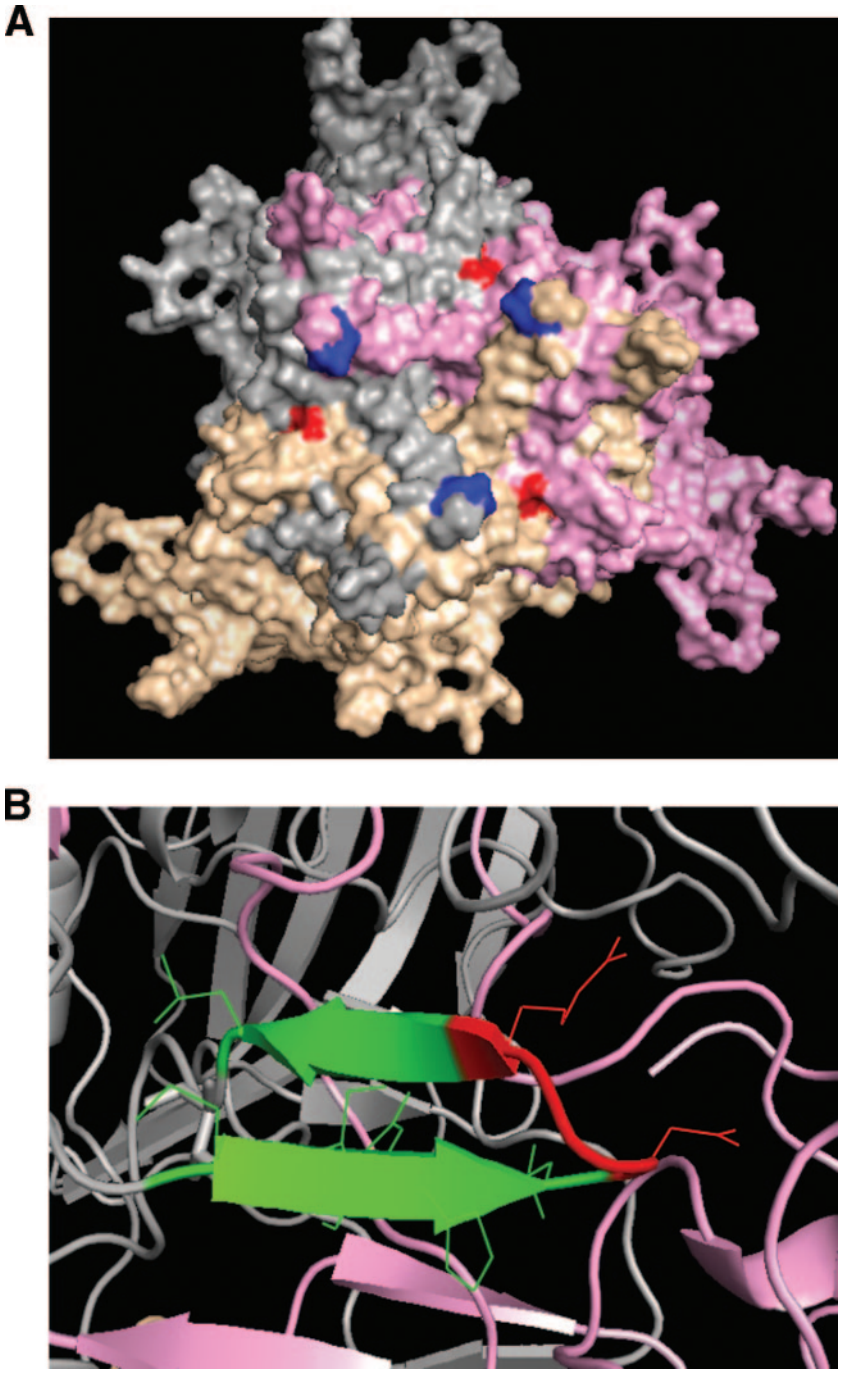

FIG. 6. (A) Three-dimensional model of an AAV2 VP3 trimer viewed down the icosahedral threefold axis of symmetry (wheat, pink, and gray). The location of the NGR integrin recognition sequence (red) is adjacent to heparin binding residues R585/R588 (blue) located within the inner loop. (B) Close-up view of the ribbon structure of the gray and pink monomers with the NGR motif (red) presented as a loop between two beta strands (green). The three-dimensional model of the AAV2 VP3 trimer was generated from VIPER with the available coordinates of AAV2 (PDB accession no. 1LP3) supplied as a template. Subsequent surface rendering was performed using PyMOL.

modification of other residues, namely N511 and G512, within the NGR domain, on the infectivity of AAV2 capsids. An N511D change, which conferred a DGR domain on AAV2, did not affect transduction in vitro in 293 cells. Interestingly, the N→D change decreased luciferase expression levels, but not the rate of onset of gene expression in mouse skeletal muscle in vivo (Asokan and Samulski, unpublished). These results suggest that the DGR motif might serve as a surrogate for the NGR domain, albeit with reduced efficiency. A recent study by Lochrie et al. included the biochemical characterization of G512A and G512P mutant AAV2 vectors (27). Both vectors displayed reduced transduction compared with that of wild-

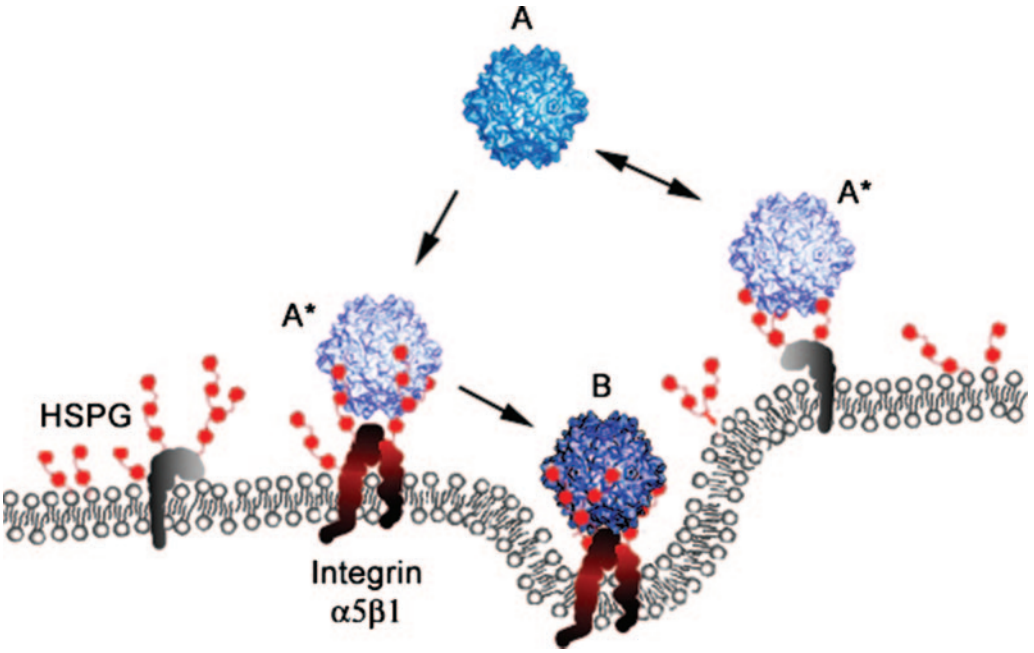

FIG. 7. Proposed "click-to-fit" model for interaction between the AAV2 capsid and α5β1 integrin. The binding of the native form of wt AAV2 (A) (blue) to cell surface heparan sulfate proteoglycans (HSPG) results in a reversible conformational change (A*) (light blue). The structurally altered virion can then detach and reattach repeatedly to different HSPG on the cell surface until the virion binds both its primary receptor (heparan sulfate) and its secondary receptor, integrin α5β1. Such cooperative interaction of the virion with heparan sulfate and integrin α5β1 results in an irreversible conformation change (B) (dark blue), which in turn could trigger endocytic uptake and subsequent viral entry.

type AAV2, with the G512P change affecting heparin binding ability, possibly due to a gross change in capsid topology. Interestingly, the modification of the NGR domain into an RGD motif produced empty AAV2 shells unable to package vector genomes (Asokan and Samulski, unpublished). This phenotype could likely arise due to the disruption of interactions between the NGR loop and the D431-R432 region, with R432 previously described as being critical for genome packaging (46).

A model for AAV2 capsid-integrin α5β1 interactions leading to cell entry. Although cell surface binding of AAV2 is mediated by its primary receptor, heparan sulfate, subsequent cellular uptake requires efficient interaction with a secondary receptor (21, 31, 38, 39). It is therefore likely that the NGR domain and amino acid residues implicated in heparan sulfate binding are both critical for mediating AAV2 capsid-integrin α5β1 interactions and subsequent cell entry. A model explaining the results described herein is depicted in Fig. 7. The binding of the AAV2 capsid to cell surface heparan sulfate in its native conformation results in a reversible conformational change that primes the NGR domain for integrin binding. At this time, the AAV2 particle could repeatedly bind to (and detach from) cell surface heparan sulfate proteoglycans until efficient engagement of the capsid with an integrin α5β1 receptor is achieved. Such a "click-to-fit" mechanism could then trigger an irreversible conformational change within the capsid and a cascade of events leading to endocytic uptake of AAV2.

Interestingly, a similar two-step mechanism has been proposed for reovirus, wherein the initial interaction with its primary receptor, sialic acid, is thought to promote a reversible conformational change that is a prerequisite for secondary receptor interactions (9). Another interesting analogy is the key role played by heparan sulfate in the interaction of fibronectin with integrin α5β1. Veiga et al. have demonstrated that integrin α5β1 is a facultative proteoglycan with extensive heparan sulfate glycosylation (42). Thus, fibronectin-integrin α5β1 interactions, which are thought to occur primarily through the RGD domain, appear to be complemented and stabilized by secondary interactions with the heparan sulfate chains on the integrin subunits and neighboring proteoglycans. A similar cooperative binding model involving cell surface heparan sulfate and integrin α5β1 could constitute the underlying basis of AAV2 cell entry.

ACKNOWLEDGMENTS

We thank Nina DiPrimio for help with heparin binding experiments and Chengwen Li for helpful comments in preparing the manuscript.

This study was supported by NIH research grants P01HL59412 (to M.A.-M.), P01HL51818, and P01HL66973 (to R.J.S.).

REFERENCES

1. **Bauer, J. S., J. Varner, C. Schreiner, L. Kornberg, R. Nicholas, and R. L. Juliano.** 1993. Functional role of the cytoplasmic domain of the integrin α5 subunit. J. Cell Biol. **122:**209–221.
2. **Berns, K. I., and C. Giraud.** 1996. Biology of adeno-associated virus. Curr. Top. Microbiol. Immunol. **218:**1–23.
3. **Bubeck, D., D. J. Filman, and J. M. Hogle.** 2005. Cryo-electron microscopy reconstruction of a poliovirus-receptor-membrane complex. Nat. Struct. Mol. Biol. **12:**615–618.
4. **Chiu, C. Y., P. Mathias, G. R. Nemerow, and P. L. Stewart.** 1999. Structure of adenovirus complexed with its internalization receptor, $\alpha_v\beta5$ integrin. J. Virol. **73:**6759–6768.
5. **Di Pasquale, G., B. L. Davidson, C. S. Stein, I. Martins, D. Scudiero, A. Monks, and J. A. Chiorini.** 2003. Identification of PDGFR as a receptor for AAV-5 transduction. Nat. Med. **9:**1306–1312.
6. **Do, A. T., E. Smeds, D. Spillmann, and M. Kusche-Gullberg.** 2006. Overexpression of heparan sulfate 6-*O*-sulfotransferases in human embryonic kidney 293 cells results in increased *N*-acetylglucosaminyl 6-*O*-sulfation. J. Biol. Chem. **281:**5348–5356.

7. **Esko, J. D., T. E. Stewart, and W. H. Taylor.** 1985. Animal cell mutants defective in glycosaminoglycan biosynthesis. Proc. Natl. Acad. Sci. USA **82:**3197–3201.
8. **Esko, J. D., J. L. Weinke, W. H. Taylor, G. Ekborg, L. Roden, G. Anantharamaiah, and A. Gawish.** 1987. Inhibition of chondroitin and heparan sulfate biosynthesis in Chinese hamster ovary cell mutants defective in galactosyltransferase I. J. Biol. Chem. **262:**12189–12195.
9. **Fernandes, J., D. Tang, G. Leone, and P. W. Lee.** 1994. Binding of reovirus to receptor leads to conformational changes in viral capsid proteins that are reversible upon virus detachment. J. Biol. Chem. **269:**17043–17047.
10. **Filardo, E. J., P. C. Brooks, S. L. Deming, C. Damsky, and D. A. Cheresh.** 1995. Requirement of the NPXY motif in the integrin beta 3 subunit cytoplasmic tail for melanoma cell migration in vitro and in vivo. J. Cell Biol. **130:**441–450.
11. **Gao, G., L. H. Vandenberghe, and J. M. Wilson.** 2005. New recombinant serotypes of AAV vectors. Curr. Gene Ther. **5:**285–297.
12. **Graham, K. L., P. Halasz, Y. Tan, M. J. Hewish, Y. Takada, E. R. Mackow, M. K. Robinson, and B. S. Coulson.** 2003. Integrin-using rotaviruses bind α2β1 integrin α2 I domain via VP4 DGE sequence and recognize αXβ2 and αVβ3 by using VP7 during cell entry. J. Virol. **77:**9969–9978.
13. **Graham, K. L., W. Zeng, Y. Takada, D. C. Jackson, and B. S. Coulson.** 2004. Effects on rotavirus cell binding and infection of monomeric and polymeric peptides containing α2β1 and αxβ2 integrin ligand sequences. J. Virol. **78:**11786–11797.
14. **Hewat, E. A., E. Neumann, J. F. Conway, R. Moser, B. Ronacher, T. C. Marlovits, and D. Blaas.** 2000. The cellular receptor to human rhinovirus 2 binds around the 5-fold axis and not in the canyon: a structural view. EMBO J. **19:**6317–6325.
15. **Humphries, M. J.** 1996. Integrin activation: the link between ligand binding and signal transduction. Curr. Opin. Cell Biol. **8:**632–640.
16. **Hynes, R. O.** 2002. Integrins: bidirectional, allosteric signaling machines. Cell **110:**673–687.
17. **Jackson, T., W. Blakemore, J. W. Newman, N. J. Knowles, A. P. Mould, M. J. Humphries, and A. M. King.** 2000. Foot-and-mouth disease virus is a ligand for the high-affinity binding conformation of integrin α5β1: influence of the leucine residue within the RGDL motif on selectivity of integrin binding. J. Gen. Virol. **81:**1383–1391.
18. **Jackson, T., A. P. Mould, D. Sheppard, and A. M. King.** 2002. Integrin αvβ1 is a receptor for foot-and-mouth disease virus. J. Virol. **76:**935–941.
19. **Jackson, T., A. Sharma, R. A. Ghazaleh, W. E. Blakemore, F. M. Ellard, D. L. Simmons, J. W. Newman, D. I. Stuart, and A. M. King.** 1997. Arginine-glycine-aspartic acid-specific binding by foot-and-mouth disease viruses to the purified integrin αvβ3 in vitro. J. Virol. **71:**8357–8361.
20. **Kaludov, N., K. E. Brown, R. W. Walters, J. Zabner, and J. A. Chiorini.** 2001. Adeno-associated virus serotype 4 (AAV4) and AAV5 both require sialic acid binding for hemagglutination and efficient transduction but differ in sialic acid linkage specificity. J. Virol. **75:**6884–6893.
21. **Kashiwakura, Y., K. Tamayose, K. Iwabuchi, Y. Hirai, T. Shimada, K. Matsumoto, T. Nakamura, M. Watanabe, K. Oshimi, and H. Daida.** 2005. Hepatocyte growth factor receptor is a coreceptor for adeno-associated virus type 2 infection. J. Virol. **79:**609–614.
22. **Kern, A., K. Schmidt, C. Leder, O. J. Muller, C. E. Wobus, K. Bettinger, C. W. Von der Lieth, J. A. King, and J. A. Kleinschmidt.** 2003. Identification of a heparin binding motif on adeno-associated virus type 2 capsids. J. Virol. **77:**11072–11081.
23. **Koivunen, E., D. A. Gay, and E. Ruoslahti.** 1993. Selection of peptides binding to the $\alpha_5\beta_1$ integrin from phage display library. J. Biol. Chem. **268:**20205–20210.
24. **Koivunen, E., B. Wang, and E. Ruoslahti.** 1994. Isolation of a highly specific ligand for the $\alpha_5\beta_1$ integrin from a phage display library. J. Cell Biol. **124:**373–380.
25. **Kornblihtt, A. R., K. Umezawa, K. Vibe-Pedersen, and F. E. Baralle.** 1985. Primary structure of human fibronectin: differential splicing may generate at least 10 polypeptides from a single gene. EMBO J. **4:**1755–1759.
26. **Li, E., S. L. Brown, D. G. Stupack, X. S. Puente, D. A. Cheresh, and G. R. Nemerow.** 2001. Integrin αvβ1 is an adenovirus coreceptor. J. Virol. **75:**5405–5409.
27. **Lochrie, M. A., G. P. Tatsuno, B. Christie, J. W. McDonnell, S. Zhou, R. Surosky, G. F. Pierce, and P. Colosi.** 2006. Mutations on the external surfaces of adeno-associated virus type 2 capsids that affect transduction and neutralization. J. Virol. **80:**821–834.
28. **Nemerow, G. R.** 2000. Cell receptors involved in adenovirus entry. Virology **274:**1–4.
29. **Opie, S. R., K. H. Warrington, Jr., M. Agbandje-McKenna, S. Zolotukhin, and N. Muzyczka.** 2003. Identification of amino acid residues in the capsid proteins of adeno-associated virus type 2 that contribute to heparan sulfate proteoglycan binding. J. Virol. **77:**6995–7006.
30. **Plow, E. F., T. A. Haas, L. Zhang, J. Loftus, and J. W. Smith.** 2000. Ligand binding to integrins. J. Biol. Chem. **275:**21785–21788.
31. **Qing, K., C. Mah, J. Hansen, S. Zhou, V. Dwarki, and A. Srivastava.** 1999. Human fibroblast growth factor receptor 1 is a co-receptor for infection by adeno-associated virus 2. Nat. Med. **5:**71–77.
32. **Rabinowitz, J. E., F. Rolling, C. Li, H. Conrath, W. Xiao, X. Xiao, and R. J. Samulski.** 2002. Cross-packaging of a single adeno-associated virus (AAV) type 2 vector genome into multiple AAV serotypes enables transduction with broad specificity. J. Virol. **76:**791–801.
33. **Rose, J. A., J. V. Maizel, Jr., J. K. Inman, and A. J. Shatkin.** 1971. Structural proteins of adenovirus-associated viruses. J. Virol. **8:**766–770.
34. **Sanlioglu, S., P. K. Benson, J. Yang, E. M. Atkinson, T. Reynolds, and J. F. Engelhardt.** 2000. Endocytosis and nuclear trafficking of adeno-associated virus type 2 are controlled by Rac1 and phosphatidylinositol-3 kinase activation. J. Virol. **74:**9184–9196.
35. **Schreiner, C. L., J. S. Bauer, Y. N. Danilov, S. Hussein, M. M. Sczekan, and R. L. Juliano.** 1989. Isolation and characterization of Chinese hamster ovary cell variants deficient in the expression of fibronectin receptor. J. Cell Biol. **109:**3157–3167.
36. **Smith, A. E., and A. Helenius.** 2004. How viruses enter animal cells. Science **304:**237–242.
37. **Stewart, P. L., C. Y. Chiu, S. Huang, T. Muir, Y. Zhao, B. Chait, P. Mathias, and G. R. Nemerow.** 1997. Cryo-EM visualization of an exposed RGD epitope on adenovirus that escapes antibody neutralization. EMBO J. **16:**1189–1198.
38. **Summerford, C., J. S. Bartlett, and R. J. Samulski.** 1999. αVβ5 integrin: a co-receptor for adeno-associated virus type 2 infection. Nat. Med. **5:**78–82.
39. **Summerford, C., and R. J. Samulski.** 1998. Membrane-associated heparan sulfate proteoglycan is a receptor for adeno-associated virus type 2 virions. J. Virol. **72:**1438–1445.
40. **Thomas, L., P. W. Chan, S. Chang, and C. Damsky.** 1993. 5-Bromo-2-deoxyuridine regulates invasiveness and expression of integrins and matrix-degrading proteinases in a differentiated hamster melanoma cell. J. Cell Sci. **105:**191–201.
41. **Triantafilou, K., Y. Takada, and M. Triantafilou.** 2001. Mechanisms of integrin-mediated virus attachment and internalization process. Crit. Rev. Immunol. **21:**311–322.
42. **Veiga, S. S., M. Elias, W. Gremski, M. A. Porcionatto, R. da Silva, H. B. Nader, and R. R. Brentani.** 1997. Post-translational modifications of $\alpha_5\beta_1$ integrin by glycosaminoglycan chains. The $\alpha_5\beta_1$ integrin is a facultative proteoglycan. J. Biol. Chem. **272:**12529–12535.
43. **Weigel-Kelley, K. A., M. C. Yoder, and A. Srivastava.** 2003. α5β1 integrin as a cellular coreceptor for human parvovirus B19: requirement of functional activation of β1 integrin for viral entry. Blood **102:**3927–3933.
44. **Wickham, T. J., E. J. Filardo, D. A. Cheresh, and G. R. Nemerow.** 1994. Integrin αvβ5 selectively promotes adenovirus mediated cell membrane permeabilization. J. Cell Biol. **127:**257–264.
45. **Wobus, C. E., B. Hugle-Dorr, A. Girod, G. Petersen, M. Hallek, and J. A. Kleinschmidt.** 2000. Monoclonal antibodies against the adeno-associated virus type 2 (AAV-2) capsid: epitope mapping and identification of capsid domains involved in AAV-2-cell interaction and neutralization of AAV-2 infection. J. Virol. **74:**9281–9293.
46. **Wu, P., W. Xiao, T. Conlon, J. Hughes, M. Agbandje-McKenna, T. Ferkol, T. Flotte, and N. Muzyczka.** 2000. Mutational analysis of the adeno-associated virus type 2 (AAV2) capsid gene and construction of AAV2 vectors with altered tropism. J. Virol. **74:**8635–8647.
47. **Xiao, X., J. Li, and R. J. Samulski.** 1998. Production of high-titer recombinant adeno-associated virus vectors in the absence of helper adenovirus. J. Virol. **72:**2224–2232.
48. **Xie, Q., W. Bu, S. Bhatia, J. Hare, T. Somasundaram, A. Azzi, and M. S. Chapman.** 2002. The atomic structure of adeno-associated virus (AAV-2), a vector for human gene therapy. Proc. Natl. Acad. Sci. USA **99:**10405–10410.